Taken from doctoral thesis, *Chemical Kinetics and Microphysics of Atmospheric Aerosols*, © copyright by James W. Morris, 2002.

# Chapter 2

# The aerosol mass spectrometer – flowtube apparatus

The increasing importance of aerosols to our understanding of air pollution problems and climate change has lead to rapid advances in instrumentation in recent years. The Aerosol Mass Spectrometer (AMS) was developed in part by our group, for aerosol composition and size measurements in the laboratory and in the field. This section describes the operational principles of the device and presents results of experiments characterizing some of its detection properties. Here, we also provide an overview of instrumentation used in these studies, including the Constant Output Atomizer used for aerosol generation, the Differential Mobility Analyzer (DMA) used for aerosol sizing, and the Condensation Particle Counter (CPC) used to measure aerosol number densities. A schematic diagram of the apparatus is shown in fig. 2-1. Description of the components and operating principles follows.

## 2.1 Aerosol generation, size selection, and counting

The AMS – Flowtube apparatus is shown in fig. 2-1, where it is shown configured for aerosol kinetics studies (ch. 5). Only minor modifications are required for microphysics studies (ch. 6). In this section we describe components of the apparatus used for aerosol generation, size selection and counting.

Taken from doctoral thesis, *Chemical Kinetics and Microphysics of Atmospheric Aerosols*, © copyright by James W. Morris, 2002.

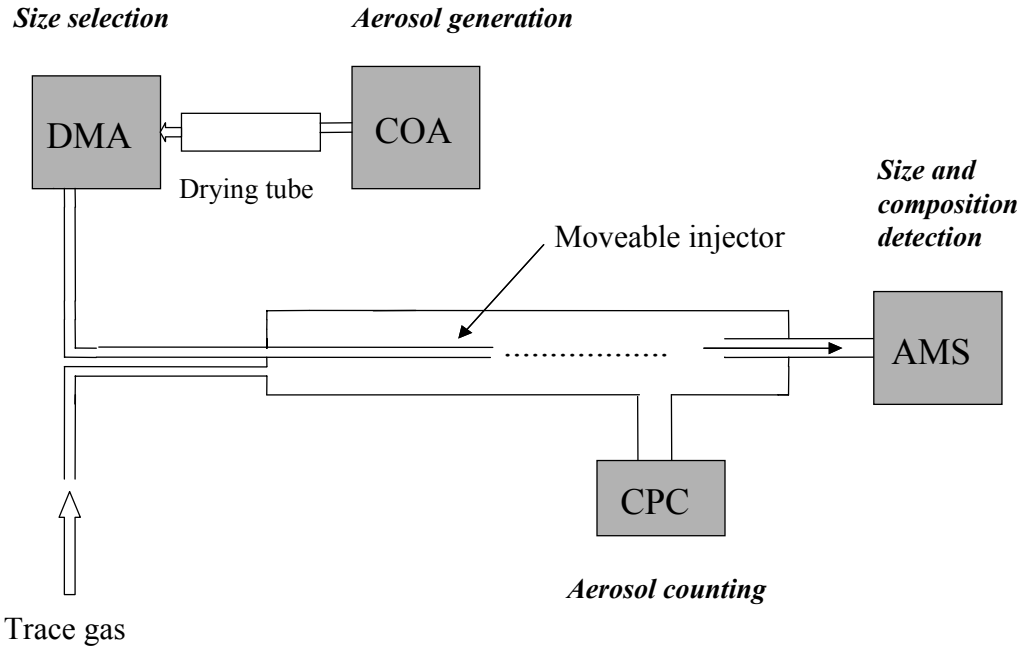


**Figure 2-1:** The AMS-Flowtube apparatus.

**The Constant Output Atomizer (COA)**

Aerosol particles for many of these studies were generated from a Constant Output Atomizer (COA, TSI Model 3075). Aerosols of a given composition are formed from atomizing a solution of the species of interest dissolved in an appropriate solvent (typically water for salt particles and methanol for organic particles). The solution is entrained into a spray region where droplets beyond a certain size (typically diameters > 100 microns) impact a collector that empties back into the solution[1]. The remaining droplets are entrained into an aerosol drier (typically a silica gel matrix) where the solvent is allowed to evaporate. Once "dried", the

particles are entrained into the apparatus for size selection, experimental processing, and detection.

**The Differential Mobility Analyzer (DMA)**

The DMA (TSI Model 3017) selects aerosols of a given size by differentiating the electrical mobility of one aerosol from another. The device consists of two concentric cylinders between which an electric field is established. Polydisperse aerosols are allowed to flow along the inside of the outer cylinder, and due to their very low diffusion coefficients, do not mix into the region between the two cylinders in the absence of an electric field. However, since the aerosols are charged at production, an electric field will exert a force on the particles directed radially inward. It can be shown that particles under the influence of such fields accelerate very rapidly to a given terminal velocity, a function of the drag force experienced by a particle of a given size[2]. Therefore, knowing the dimensions of the cylinders, the number of charges on the particles, and the diameter of the particle of interest, the magnitude of the electric field can be chosen such that the selected particle passes through a small opening in the center cylinder for selection. The selected particles have a radial drift time (due to the electric field) equal to the vertical flow time along the cylinders. All other particles either impact the inner cylinder or are entrained out, by passing the selection opening.

**The Condensation Particle Counter (CPC)**

The CPC is used to count the number density of particles using optical detection[3]. Particles pass between a light source and a detector sensing the particle's shadow. The CPC 3010 is sensitive to particles having diameters greater than typically 10

nm. These particles must be altered for detection since light used in this device has a wavelength closer to 1000 nm. This is accomplished through a butanol condenser. The particles are sampled into a region supersaturated in butanol vapor such that they grow by condensation before detection in the optical chamber of the device.

**The Laminar Flowtube**

Each component is connected in line to the aerosol flowtube (diameter = 1.092 cm). For flows (1 L/min) and pressures (1 atm) typical in these studies, flow conditions are laminar (Reynolds number << 2000) up to the moment of sampling. This is especially important in the aerosol kinetics study for which the flow conditions are described in detail in ch. 5.

## 2.2 The Aerosol Mass Spectrometer (AMS)

Here we summarize the basic features of the AMS. The detailed operation of the device can be found in *Jayne et al.,* [2000][4]. The AMS (Fig. 2-2) utilizes a recently developed aerodynamic focusing lens[5] to maximize particle transmission into the vacuum chamber where particles are vaporized and detected. The pressures at the lens entrance and exit are about 2 torr and $10^{-3}$ torr respectively. The pressure difference accelerates the aerosols through the lens, imparting velocities as a function of aerosol aerodynamic diameter (the diameter of a unit density sphere having the same settling velocity). The lens focuses the particles into a narrow beam (~1/2 mm and 1 mm in diameter for liquid and solid particles respectively), directed into the first of three differentially pumped chambers. The pressures in the

Taken from doctoral thesis, *Chemical Kinetics and Microphysics of Atmospheric Aerosols*, © copyright by James W. Morris, 2002.

second and third chambers are $10^{-5}$ torr and $10^{-7}$ torr respectively, such that each particle maintains its velocity as it traverses the chambers. In the third chamber the particles strike a resistively heated surface where the aerosols vaporize in 20 to 200 microseconds depending on particle composition and heater temperature. The vapor plume is ionized by electron impact and the resulting ions are mass analyzed with a quadrupole mass spectrometer (UTI Model 100C).

Taken from doctoral thesis, *Chemical Kinetics and Microphysics of Atmospheric Aerosols*, © copyright by James W. Morris, 2002.

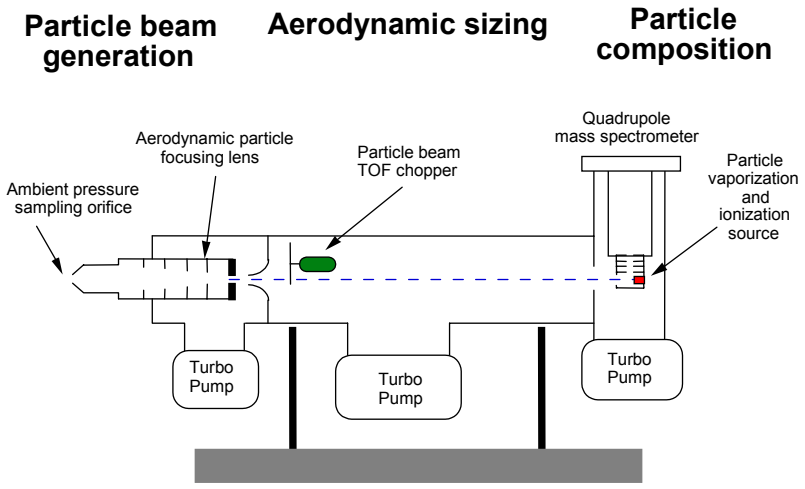


**Figure 2-2:** The aerosol mass spectrometer used for particle size and composition measurements.

A two-slit chopper wheel positioned near the exit of the focusing lens intercepts the particle beam producing pulses of particles for time of flight (TOF) analysis. Typically the chopper rotates at 70 Hz with a 1.7% duty cycle. The TOF is determined by the elapsed time (~$10^{-3}$ s) between the trigger pulse signaling the chopper opening and the ion pulse due to the vaporized aerosol. The ion signal is stored in a time-calibrated bin with 10 μs time steps. TOF can be converted to particle aerodynamic diameter, which for spherical particles is the product of the specific gravity and the geometric diameter (see ch. 3).

The AMS can be operated in either of two modes: In the TOF mode, signal proportional to the mass of the particles is monitored as a function of TOF or

aerodynamic diameter (see sec. 3.3) for a given atomic mass unit (AMU). In the mass spectrum mode, the entire mass spectrum of the particles is displayed from 1 to 300 AMU. The TOF signal can be processed in both a single particle mode and in an integrated signal mode.

## 2.3 The aerodynamic focusing lens

### 2.3.1 Operating principle

Prior aerosol mass spectrometers[6] were largely limited by their ability to focus aerosols into a beam with a sufficiently small radius for effective detection. The AMS used in these studies utilizes a newly developed aerodynamic focusing lens[7], allowing aerosols to be focused into a beam ~1 mm in diameter, such that very few particles sampled into the instrument escape detection. The beam focuses the particles by creating a tightly focused air beam within the lens that particles over a wide range of sizes can follow. When the air beam exits the lens into $10^{-3}$ torr, most of the air molecules diverge. However, due to their relatively large momentum compared to the air molecules, particles with velocity components aligned with the lens axis tend to continue along a straight-line path to detection. Large (> 1 micron) particles have a tendency to deviate from the air stream path within the lens and can impact the lens walls. Conversely, small (< 100 nm) particles tend to follow the air beam so well that upon exiting the lens they can diverge with the gas molecules. In this section we discuss a method for measuring this small particle loss. Later, we will use the measured particle transmission efficiency in an analysis of size distributions representing coagulating sulfuric acid aerosols (see ch. 6).

Taken from doctoral thesis, *Chemical Kinetics and Microphysics of Atmospheric Aerosols*, © copyright by James W. Morris, 2002.

### 2.3.2 Measurement of the transmission efficiency

In principle, measuring the transmission of particles of a given size is straightforward. One samples air containing particles of a single size into the AMS while simultaneously sampling the same air into a separate particle counter, such as a Condensation Particle Counter (CPC, TSI Model 3010). The ratio of the AMS counts to CPC counts gives the transmission efficiency at that size. For example, polystyrene latex (PSL) spheres of given sizes are commercially available and can be used to create a suspension in water for use in the atomizer. This suspension can then be used to generate particles to be sampled into the AMS and the CPC. However, PSL spheres are not presently available in pure water, and concentrations of other particles, or even salts within the water (which upon drying form particles), will lead to over-counts at the CPC (since more than the PSL's are being counted). The AMS can be tuned to a single m/z (i.e. for PSL spheres) such that one counts only the particles of interest, but the CPC will count all particles size-selected by the DMA. This is especially problematic for particles of interest here, with diameters under 100 nm, as most contaminants result in particles in this range. To circumvent this problem, we have designed a novel technique for measuring small particle transmission efficiencies using a poly-disperse particle size distribution of spherical particles and the DMA (TSI Model 3071A). Here we present a conceptual overview of the technique only. Exact expressions used can be found in cited references when necessary.

The DMA selects particles on the basis of the particle's charge and mobility diameter[2]. More specifically, the DMA selects all positively charged particles with a given terminal velocity under an applied electric field. For particles of charge $q$, with

radius $a$, moving through a gas at terminal velocity $v$, under the influence of an electric field $E$, feeling a drag force, $F_{drag}$, Newton's law is expressed as:

$$\vec{F}_{net} = q\vec{E} - \vec{F}_{drag}(a,\vec{v}) = m\vec{a} = 0 \qquad (2.1)$$

From eq. 2.1[a], we can solve for the terminal velocity. However, particles sampled into the DMA have multiple charges (mostly 1, 2 and 3), and degenerate terminal velocities for particles of different sizes are possible. Since eq. 2.1 is nonlinear with no analytical solution, we used the Newton-Raphson method[8] to numerically solve for the sizes sharing the same terminal velocities as a function of $q$. This allows prediction of all the sizes that will result from a given mobility size-selection from the DMA. The fraction of the particles with a given charge can also be predicted if a Boltzmann equilibrium distribution of charges prevails. A Boltzmann distribution can typically be achieved through the use of charge neutralizers in line with the DMA. Using the Boltzmann law (for any equilibrium microcannonical ensemble)[9], we may express the fraction of particles in an ensemble having charge $q$ and radius $a$, under such conditions as:

$$f(q,a) = \frac{\exp(\frac{-V(q,a)}{k_B T})}{\sum_{i=1}^{\infty} \exp(\frac{-V(q_i,a)}{k_B T})} \qquad (2.2)$$

In this expression, $V(q,a)$ is the potential energy of (or electrostatic work required to build) a particle of radius $a$ with $q$ charges attached. Equations 2.1 and 2.2 enable us to predict both the particle diameters and relative fractions (of the total area of the mass distribution) of each size selected by the DMA. Fig. 2-3 shows DMA output as sampled by the DMA with model prediction lines plotted from theory. Oleic acid was used for

[a] The exact expression for the drag force assumes a corrected Stokes drag and can be found in Seinfeld and Pandis, 1998.

Taken from doctoral thesis, *Chemical Kinetics and Microphysics of Atmospheric Aerosols*, © copyright by James W. Morris, 2002.

these studies. Having predicted the relative fractions of each mode, we measured the small particle transmission by decreasing the selected size-1 diameter until the model no longer matched the observed mode fraction. The transmission efficiency will be given by the ratio of the observed to predicted mode intensities (a ratio of masses at the same size equals a ratio of numbers at that size). The observed mode intensity is taken as the integral under the curve for a given mode. Once the transmission efficiency (< 1) for a given size is known, it can then be chosen as size-3, for example, allowing measurement of transmission efficiencies for sizes 1 and 2.

Taken from doctoral thesis, *Chemical Kinetics and Microphysics of Atmospheric Aerosols*, © copyright by James W. Morris, 2002.

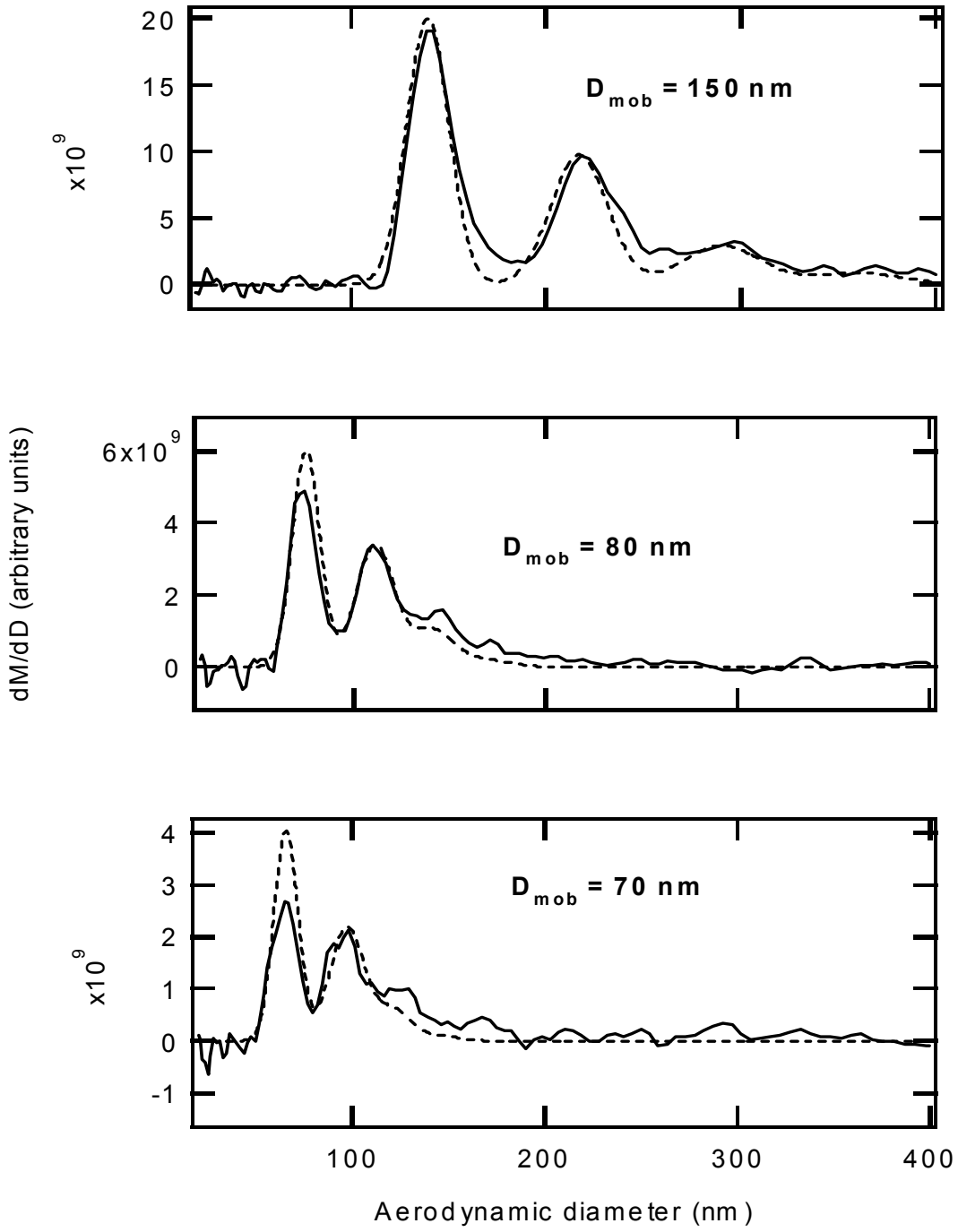


**Figure 2-3:** Raw data used to calculate the transmission efficiency as a function of aerodynamic diameter. The 150 nm data shows the model accuracy in the case where transmission is unity. The 80 nm and 70 nm plots show a transmission of 0.8 and 0.6 respectively.

Varying the selected mobility diameters in this way, one can measure the transmission as a function of aerodynamic diameter (specific gravity times the mobility diameter), shown in fig. 2-4. The function used in the curve fit shown has the following form:

$$\varepsilon(D_{aero}) = 1 - \exp(\frac{-(D_{aero} - D_{crit})^2}{\beta^2}) \tag{2.3}$$

Here ε represents the transmission efficiency. This formulation for ε has a domain defined by, $D_{crit} < D_{aero} < D_{max}$. The upper end of the domain marks the region where large particle transmission falls beneath unity, requiring a different functional form. Since corrections to observed size distributions go as the inverse of the transmission efficiency, the reliability of this function breaks down as $D_{aero}$ approaches $D_{crit}$. In this limit one makes a correction many times larger than the accuracy of the measurement. When correcting distributions, it is advisable to work in raw data (TOF) space. Writing ε(TOF) is straightforward given $D_{aero}$(TOF) (see ch. 3).

Taken from doctoral thesis, *Chemical Kinetics and Microphysics of Atmospheric Aerosols*, © copyright by James W. Morris, 2002.

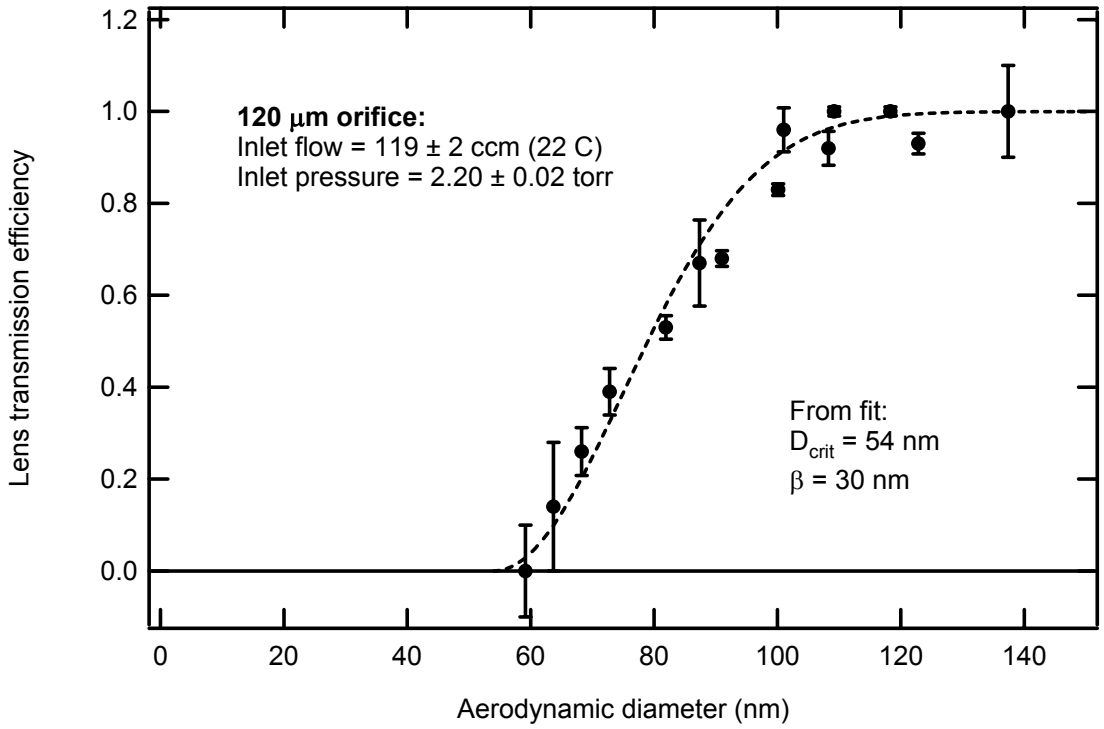


**Figure 2-4**: Small particle lens transmission efficiency as a function of aerodynamic diameter.

### 2.3.3 Estimation of the gas temperature at the lens exit

As previously described, the particles are sampled from atmospheric pressure through a pinhole whose diameter is approximately 100 μm. The pressure in this first volume is near 2 torr. The volume in the 2 torr region is on the order of 10 cc and the flow rate into the instrument is near 2 cc/s (~ 800 cc/s within the 2 torr region). This means that particles spend on the order of $10^{-2}$ s within the 2 torr region before entering the first lens orifice. Passage through the lens is more rapid and at much lower pressures. In this case

the gas is not expected to be in thermal equilibrium with the walls of the lens and some cooling of the particles may occur through evaporation. In addition, there may be cooling of the gas molecules as they are focused axially within the lens. Here, we describe the basic physics behind this gas phase cooling before attempting to measure it with an indirect method. These results are expected to be important for modeling expected water loss from particles as they are sample into the AMS.

The cooling described here is to be distinguished from a throttling process in which the gas undergoes adiabatic compression and expansion[10]. In a throttling process a volume of air is compressed as it passes through an orifice. If the volume flow rate on the high pressure side is $dV/dt$, then $PdV$ Joules of work are done on the gas (in a period of time, $dt$) as it enters the orifice, and $P'dV'$ are done by the gas on its surroundings as it expands coming out the other side. For an ideal gas undergoing an adiabatic process, $dQ = 0$, and conservation of energy with the first law of thermodynamics allows[11]:

$$C_v dT + pdV = dQ = 0 \qquad (2.4)$$

Here $C_v$ is the heat capacity of the gas at constant volume $(dU/dT)_v$. Since for a throttling process the net $PV$ work is zero, it follows that the temperature change is zero as well. Our assumption that the process is adiabatic follows from the premise that the compression and expansion is too rapid for heat to flow into the gas from the surroundings (lens wall). This of course is quite different from the case where a gas is simply allowed (or made) to expand into a region of lower pressure under adiabatic

conditions. In such a case the cooling is established by virtue of the work the gas has done on its surroundings[b].

In the case of a low-pressure gas flowing through several small orifices, the physics is more complicated. Because of the very low pressure, the problem is perhaps best dealt with on the level of molecular dynamics, rather than through thermodynamics or even fluid dynamics. Here, we describe the conceptual justification for one way the beam of molecules might be cooled as it exits the lens. Since the gas streamlines are increasingly focused, the component of their velocities in the axial direction is increasing as they near the lens exit. Upon exiting the final orifice a situation obtains wherein fast molecules collide with slower ones, simultaneously slowing the fast ones and increasing the speed of the slow ones. This effect serves to sharpen the velocity distribution, and thereby decreases the temperature of the gas within the air beam.

Here we will describe a method enabling indirect measurement of the temperature of the air beam after having exited the aerodynamic focusing lens. Although the AMS was designed to measure aerosol mass fluxes as a function of time of flight (TOF), it can also detect signal from the gas molecules for which the velocities are sufficiently axially oriented. Such detection enables us to measure the velocity distribution of the gas-phase species. Since the measured signal is from a molecular beam, we have to account for the beam velocity. This represents the air speed upon exiting the orifice and establishes an upper limit for small particle velocities. We will gain information about the air beam temperature through the spread in velocities assuming they follow a Boltzmann

[b] The same cooling leads to the atmospheric lapse rate which one can show from thermodynamics to be –10 C / kilometer.

distribution in the axial ($x$) direction. The Boltzmann velocity distribution along one axis is given by[12]:

$$f(v_x) = \left(\frac{m}{2\pi k_B T}\right)^{1/2} \exp\left(\frac{-mv_x^2}{2k_B T}\right) \tag{2.5}$$

Equation 2.5 is the probability density that a molecule will have the $x$-component of its velocity between $v_x$ and $v_x + dv_x$ (the fraction of such molecules is given by $f(v_x)dv_x$).

In the case of a molecular beam with drift velocity $v_d$, we need only translate the reference frame of this expression to the right by that amount:

$$f(v_x) = \left(\frac{m}{2\pi k_B T}\right)^{1/2} \exp\left(\frac{-m(v_x - v_d)^2}{2k_B T}\right) \tag{2.6}$$

We may now use this expression to fit the signal distribution in velocity space. In this case, signal proportional to mass also allows signal proportional to number since all molecules (of a given m/z) have the same size. Were one to normalize the signal, a true probability density would be obtained. Knowing the mass of the species, we extract $T$ and $v_d$ from the fit.

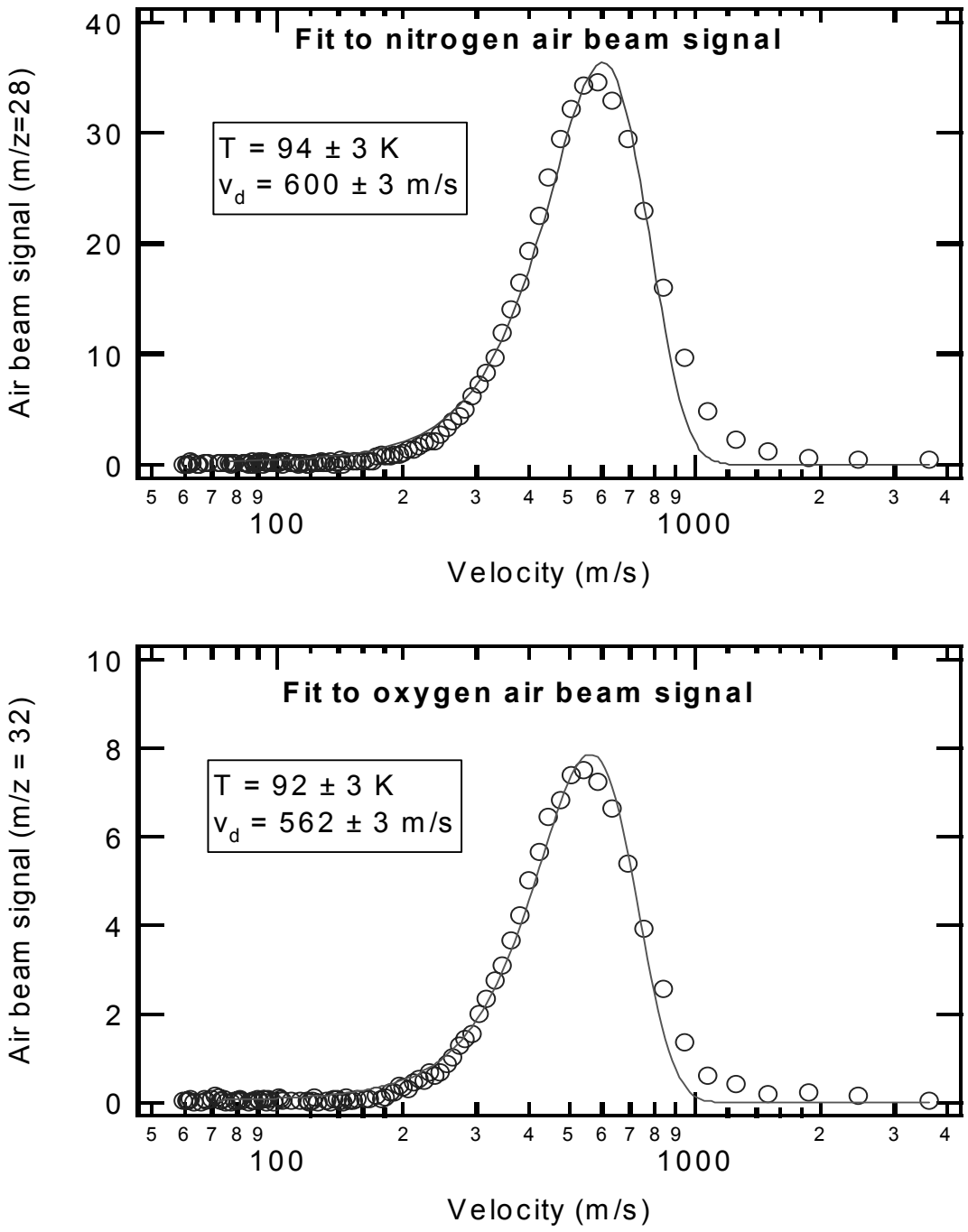


**Figure 2-5**: One dimensional Boltzmann velocity distribution fits to AMS nitrogen and oxygen air beam signals.

Taken from doctoral thesis, *Chemical Kinetics and Microphysics of Atmospheric Aerosols*, © copyright by James W. Morris, 2002.

The fits are shown in fig. 2-5. Fits to both nitrogen and oxygen yield a consistent temperature of around 93 degrees Kelvin, or –180 degrees Celsius. This substantial cooling will have potential implications for the particle evaporation rate and phase, but it is a question for future work to model to what extent this cooling affects the temperature of the aerosols. It is noteworthy that the shape of the function does not match that of the signal for higher velocities. This non-Boltzmann character may be due to lens / air beam interactions that are neglected here. It is also of note that the heavier oxygen air beam is moving about 6% slower than the nitrogen air beam. These fits are also consistent with data for Argon (not shown) for which $v_d$ and $T$ were found to be 574 m/s and 92 K respectively.

## 2.4 Particle beam widths as an indicator of aerosol phase

The AMS not only delivers quantitative information of a particle's size and composition, it can also indicate the phase of a particle. A particle that undergoes a change of phase from liquid to solid generally loses its sphericity. Non-sphericity not only changes the drag force on a particle, changing its aerodynamic diameter, but it also can lead to so-called lift forces that affect the way the particles exit the lens. This in turn affects the width (number density as a function of radial position) of the particle beam exiting the lens. In an ideal situation, a beam width could be correlated with an extent of solidification or phase diagram for mixtures of species with varying melting points. Little work has been done to explore this AMS feature, however, and the data presented here are meant only to motivate future research. Early investigations showed the beam widths of dioctylpthalate (DOP) and other oils to be approximately 0.5 mm in diameter,

Taken from doctoral thesis, *Chemical Kinetics and Microphysics of Atmospheric Aerosols*, © copyright by James W. Morris, 2002.

as measured by a translatable wire located just downstream of the chopper. This was in contrast to ammonium nitrate and other salts whose particle beam diameters were measured to be more like 1 mm in diameter[3].

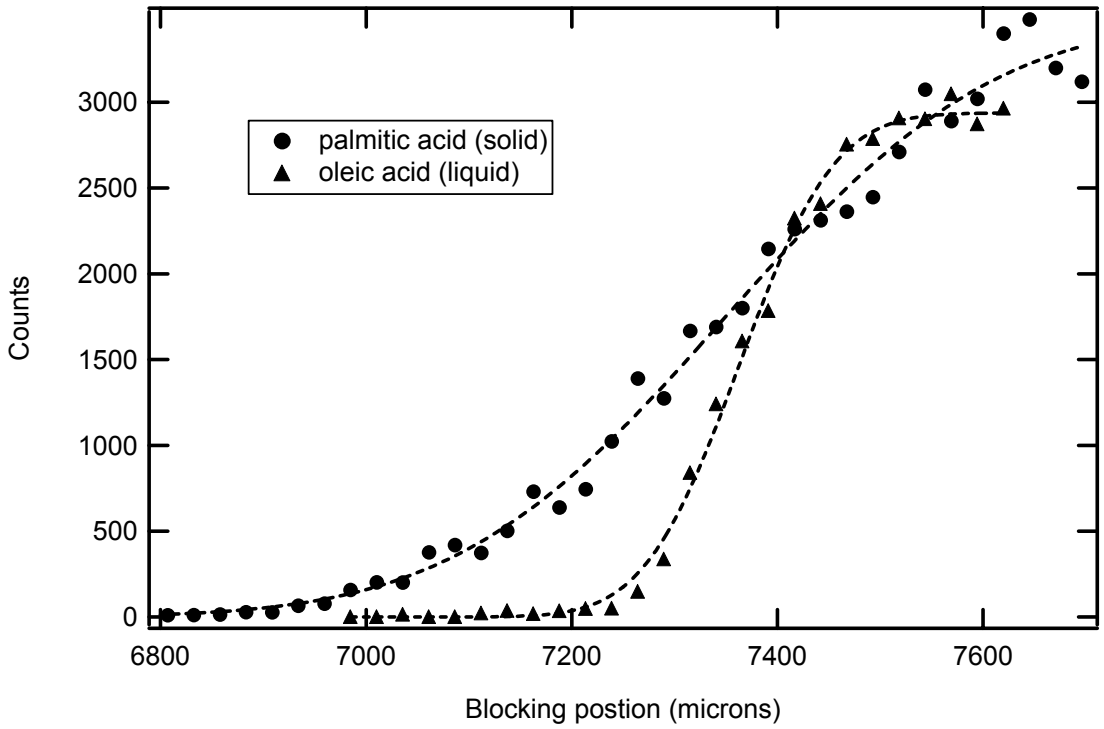


**Figure 2-6**: Beam width measurement for palmitic and oleic acids. The width at half maximum counts gives beam widths of 0.4 and 0.3 mm respectively.

Here we show results on pure oleic and palmitic acids. Palmitic acid is a solid at room temperature. In these experiments a translatable plate was used instead of a wire, and the count rate as a function of the occlusion was fit to an Error function (integrated Gaussian).

## Chapter 2 References

[1] TSI Model 3075/3076 Constant Output Atomizer, *Instruction Manual*, 1996.

[2] TSI Model 3071A Electrostatic Classifier, *Instruction Manual*, 1998.

[3] TSI Model 3010 Condensation Particle Counter, *Instruction Manual*, 1996.

[4] J. Jayne, D. Leard, Z. Zhang, P. Davidovits, C. Kolb, and D. Worsnop. *Aerosol Sci. Technol*., **33**, 49 (2000).

[5] P. Liu, P. J. Ziemann, D. B. Kittelson, and P. H. McMurry, *Aerosol Sci. Technol*., **22**, 293 (1995a).

[6] M. P. Sinha, C. E. Griffin, D. D. Norris, T. J. Estes, V. L. Vilker, S. K. Friedlander, *J. Colloid and Interface Science*, **87**, 140 (1982).

[7] P. Liu, P. J. Ziemann, D. B. Kittelson, P. H. McMurry, *Aerosol Sci. Technol*., **22**, 314 (1995b).

[8] W. Press, *Numerical Recipes in C*, (Cambridge University Press, Cambridge, 1992).

[9] F. Reif, *Fundamentals of Statistical and Thermal Physics*, (McGraw-Hill, Boston, 1965, 131).

[10] Reif, p. 204.

[11] E. Fermi, *Thermodynamics*, (Dover, New York, 1936, 87).

[12] P. Atkins, *Physical Chemistry, Sixth Edition*, (Freeman, New York, 1998).